PHYSICAL REVIEW B **79**, 224417 (2009)

Valence bond solid phases on deformed kagome lattices: Application to $Rb_2Cu_3SnF_{12}$

Bohm-Jung Yang[1] and Yong Baek Kim[1,2]
[1]*Department of Physics, University of Toronto, Toronto, Ontario, Canada M5S 1A7*
[2]*School of Physics, Korea Institute for Advanced Study, Seoul 130-722, Korea*
(Received 2 March 2009; revised manuscript received 13 May 2009; published 12 June 2009)

Motivated by a recent experiment on $Rb_2Cu_3SnF_{12}$, where spin-1/2 Cu^{2+} moments reside on the layers of kagome-like lattices, we investigate quantum ground states of the antiferromagnetic Heisenberg model on a series of deformed kagome lattices. The deformation is characterized by a weaker exchange coupling αJ on certain lattice links appropriate for $Rb_2Cu_3SnF_{12}$ with $\alpha=1$ corresponding to the ideal kagome lattice. In particular, we study possible valence bond solid phases using the perturbation theory around isolated dimer limits, dimer series expansion, and self-consistent bond operator mean-field theory. It is shown that the valence bond solid phase with a 36-site unit cell of the ideal kagome lattice is quite sensitive to a small lattice distortion as the kind discovered in $Rb_2Cu_3SnF_{12}$. As a result, we find that a more likely quantum ground state in $Rb_2Cu_3SnF_{12}$ is the valence bond solid phase with a 12-site unit cell, where six dimers form a pinwheel structure, leading to strong modification of the elementary triplet and singlet excitation spectra in the deformed kagome lattices.

DOI: 10.1103/PhysRevB.79.224417 PACS number(s): 74.20.Mn, 74.25.Dw

I. INTRODUCTION

Lattice distortions are abundant in frustrated magnets as they are efficient ways to relieve the frustration and lift the macroscopic degeneracy of the classical ground states. This has been, for example, an obstacle to synthesize and study materials that can be described by the quantum Heisenberg model with spin-1/2 moments on "ideal" lattice structures with isotropic spin-exchange couplings. The interest in the ideal models stems from various theoretical suggestions for novel emergent quantum paramagnetic phases such as quantum spin liquid[1–6] and valence bond solid (VBS) (Refs. 7–10) phases. On the other hand, those deformations may lead to different kinds of emergent quantum ground states and understanding precisely how these phases are connected to the quantum ground states in the ideal limit would help us understand more global picture of the quantum frustrated magnets.[11,12]

One of the most studied frustrated magnets is the quantum spin-1/2 antiferromagnetic Heisenberg model on the kagome lattice. There exist several materials that are candidates for the realization of this system.[13–20] It has been, however, found that many materials undergo lattice deformations and quite often these lead to magnetically ordered phases at sufficiently low temperatures.[13,14] So far, there are a small number of examples of two-dimensional kagome or kagome-like materials with spin-1/2 moments that do not show any magnetic ordering down to very low temperatures.[15–20] The Herbertsmithite, $ZnCu_3(OH)_6Cl_2$,[16–18] is known for the ideal kagome lattice structure, but it suffers from intersite mixing between Cu^{2+} and Zn^{2+} and makes the interpretation of the susceptibility data difficult. In the Volborthite, $Cu_3V_2O_7(OH)_2\cdot 2H_2O$,[19] the kagome structure is deformed in an orthorhombic fashion, leading to two inequivalent spin-exchange couplings between Cu^{2+} moments. In both cases, the specific heat at low temperatures reveals the absence of (or a very small) excitation/spin gap (down to 50 mK in Herbertsmithite, for example), leading to various suggestions for exotic quantum ground states.[5,6,9] More recently, it is found that Cu^{2+} moments in $Rb_2Cu_3SnF_{12}$ form the layers of a deformed kagome lattice and do not show any magnetic order at low temperatures.[20] The susceptibility data clearly show a spin-excitation gap (in contrast to the previous two materials), which is of the order of 20 K, while the average strength of the exchange coupling is estimated to be around 200 K, which leads to the expectation that the ground state may be a VBS state.

In this paper, we investigate the quantum ground states of the spin-1/2 antiferromagnetic Heisenberg model on a series of deformed kagome lattices that may be relevant to $Rb_2Cu_3SnF_{12}$. Each deformed kagome layer can be described by four possibly different nearest-neighbor exchange couplings, labeled by J_1, J_2, J_3, and J_4 in decreasing order in magnitude as inferred from different Cu^{2+}-F^--Cu^{2+} bond angles [see Fig. 1(a)]. In $Rb_2Cu_3SnF_{12}$, J_1, J_2, and J_3 are similar in magnitude, while the magnitude of J_4 is about a

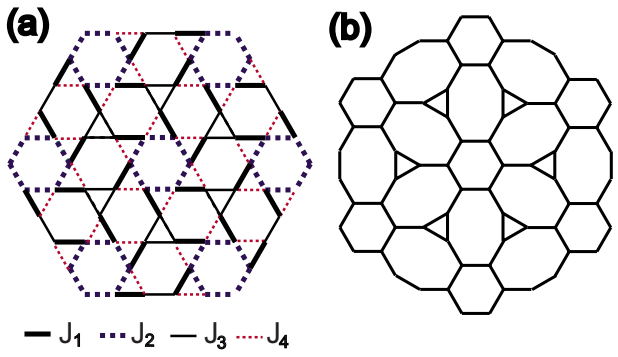

FIG. 1. (Color online) (a) The deformed kagome lattice with four different neighboring exchange interactions, which may be realized in $Rb_2Cu_3SnF_{12}$. Here all the exchange coupling constants are positive and satisfy $J_1>J_2>J_3\gg J_4$. In this work, we consider the case of $J_1=J_2=J_3=J>J_4$. (b) The J_4-depleted kagome lattice that is topologically equivalent to the deformed kagome lattice when $J_1=J_2=J_3=J$ but $J_4=0$.

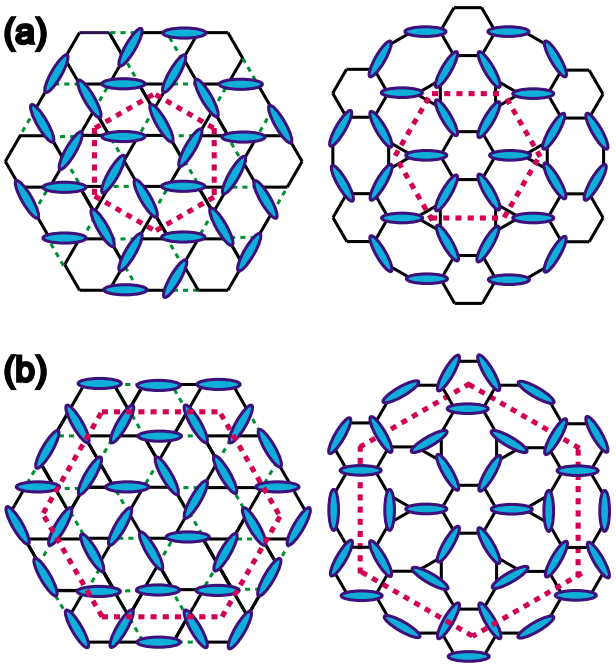

FIG. 2. (Color online) Two candidate valence bond solid configurations on the deformed kagome lattice. The figure on the left-hand side is the configuration on the original deformed kagome lattice and the picture on the right-hand side represents a topologically equivalent lattice of the J_4-depleted lattice. The light dotted (green) lines on the left-hand side pictures show the J_4 links. (a) VBS-12: a valence bond solid with a 12-site unit cell. (b) VBS-36: a valence bond solid with a 36-site unit cell. Here the thick dotted (pink) lines indicate the unit cells.

half of the others.[20] Hence it is reasonable to start from a model where $J_1=J_2=J_3=J \gg J_4$. Here we study the evolution of the quantum ground states as a function of $\alpha=J_4/J \leq 1$, where $\alpha=1$ corresponds to the ideal kagome lattice.

Using perturbative arguments starting from isolated dimer limits, we find that there exist two competing VBS phases on these lattices; one with a 12-site unit cell [VBS-12, shown in Fig. 2(a)] and another with a 36-site unit cell [VBS-36, shown in Fig. 2(b)]. The VBS-36 phase is smoothly connected to the VBS phase with a large unit cell on the ideal kagome lattice, which has been suggested as a strong contender for the quantum ground state of the spin-1/2 antiferromagnetic Heisenberg model.[7–9] The perturbation theory clearly shows that the VBS-12 is the lower-energy ground state when $\alpha=0$, namely, on the J_4-depleted lattice. On the other hand, the VBS-36 becomes the ground state when $\alpha=1$, consistent with the previous studies on the ideal kagome lattice. We study the relative stability of these phases for an arbitrary deformation parameter α using the perturbation theory, dimer series expansion, and bond operator mean-field theory. Thus our work can also test the stability of the VBS phase with a 36-site unit cell on the ideal kagome lattice against the deformation from the ideal kagome lattice structure.

It is found that the VBS-36 phase on the ideal kagome lattice is quite sensitive to the deformation, and only 3% reduction in the magnitude of J_4 is enough to induce the instability of the VBS-36 state of the ideal kagome lattice. Thus we propose that the ground state for $\alpha<0.97$ is the VBS-12 state. Note that the VBS-12 state is clearly the ground state of J_1-only model or when $J_2, J_3 \ll J_1$. It is remarkable that the VBS-12 state is stable even when the strength of J_2 and J_3 are equal to J_1. Thus we conclude that the VBS phase discovered in $Rb_2Cu_3SnF_{12}$ is most likely the VBS-12 state. In order to provide a future experimental test for the VBS-12 state, we compute the triplet dispersion spectra as shown in Fig. 3.

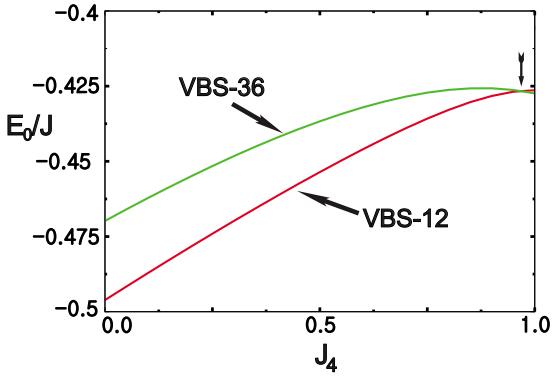

FIG. 3. (Color online) Ground-state energies of the VBS-12 and the VBS-36 phases as a function of J_4/J (J is set to one) obtained from the bond operator mean-field theory. Note that there is a level crossing around $J_4=0.97J$ as indicated by an arrow.

The rest of the paper is organized as follows. In Sec. II, we use perturbative arguments about isolated dimer limits to show that there exist two competing VBS phases—the VBS-12 and VBS-36-on the J_4-depleted lattice. In Sec. III, the dimer series expansion and the bond operator mean-field theory are developed to investigate the relative stability of the two candidate VBS phases for an arbitrary strength of J_4/J. The triplet dispersion spectra are also discussed in detail for the VBS-12 state. Finally, in Sec. IV, we discuss the implications of our results to theory and experiments.

II. VALENCE BOND SOLID GROUND STATES ON THE J_4-DEPLETED KAGOME LATTICE

A. Second-order perturbation and the VBS-12 state

We can obtain valuable information about the spatial ordering pattern of singlet dimers by applying the perturbation theory around an isolated dimer limit.[21] To perform the calculation, we divide the Hamiltonian into two parts, i.e., $H=H_0+\lambda V$. Here H_0 describes the Heisenberg spin-exchange interaction between two nearest-neighbor spins constituting a singlet dimer. The interdimer interactions are contained in V which is treated as a perturbation. The ground state of the unperturbed Hamiltonian H_0, i.e., $|\Psi_0\rangle$ can be taken as the direct product of a set of isolated dimer singlets lying on the J_4-depleted kagome lattice.

Let us start from two possible local configurations of two neighboring dimer singlets as shown in Figs. 4(a) and 4(b). Note that a pair of neighboring dimers can be aligned in parallel, connected by a single unoccupied link [Fig. 4(a)], or they can be aligned in a perpendicular direction if one end of

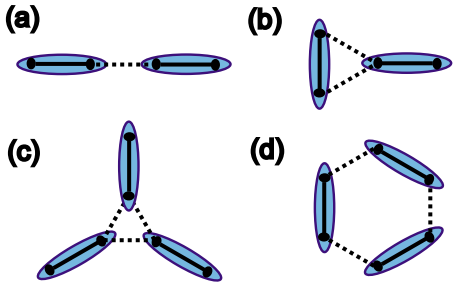

FIG. 4. (Color online) Local configurations of neighboring dimers, which contribute to the lowest-order perturbation theory. Here an ellipse indicates a dimer singlet. A solid line shows the intradimer coupling included in H_0, while a dotted line indicates the interdimer coupling contained in the perturbation, V. (a) Neighboring dimers are lying in parallel. There are energy gains $\Delta\epsilon^{(2)}=-\frac{3}{32}J\lambda^2$ in the second order and $\Delta\epsilon_a^{(3)}=-\frac{3}{128}J\lambda^3$ in the third order. (b) Neighboring dimers are lying in a perpendicular geometry. There is no energy gain in the perturbation theory (explained in the text). Here the triangle carrying a dimer is called a filled triangle. (c) An empty triangle. There is no energy gain in the third-order perturbation theory. (d) A perfect hexagon. There is an additional energy gain $\Delta\epsilon_b^{(3)}=-\frac{9}{128}J\lambda^3$ in the third-order perturbation theory.

a dimer is simultaneously connected to both spins of its neighboring dimer [Fig. 4(b)]. The important point is that the ground-state energy can be lowered through second-order perturbation processes only when the two dimers are lying in parallel. When two dimers are lying in a perpendicular direction, $V|\Psi_0\rangle=0$ because of the odd parity of the singlet state with respect to the reflection and there is no energy shift due to the second-order processes. The energy gain from each configuration where two neighboring dimers are lying in parallel is $\Delta\epsilon^{(2)}=-\frac{3}{32}J\lambda^2$.

In order to determine the global structure of the VBS phases, however, we need to take into account all the geometric constraints for possible VBS patterns. Note that the basic building blocks of the J_4-depleted kagome lattice are triangles, hexagons, and bridge links which connect each triangle to its neighboring hexagons [shown in Fig. 1(b)]. One can show that the number of triangles, N_Δ, is given by $N_\Delta=\frac{N}{6}$, where N is the number of spins (or lattice sites) on the lattice. Similarly, the number of hexagons, N_{Hexagon}, and the number of bridge links, N_{Bridge}, satisfy $N_{\text{Hexagon}}=\frac{N}{12}$ and $N_{\text{Bridge}}=\frac{N}{2}$, respectively. The total number of links, L_{Link}, on the lattice is then given by

$$N_{\text{Link}}=3N_\Delta+6N_{\text{Hexagon}}+N_{\text{Bridge}}=\frac{3}{2}N.$$

Since the number of dimers, N_{Dimer}, is equal to $\frac{N}{2}$ and each dimer is lying on a single link, the total number of the unoccupied links is $N_{\text{Link}}-N_{\text{Dimer}}=\frac{3}{2}N-\frac{1}{2}N=N$. The unoccupied links connecting neighboring dimers in various local dimer configurations are shown as the dotted lines in Fig. 4

According to the result of the second-order perturbation theory for two neighboring dimers, when one of the links of a triangle is occupied by a dimer singlet (we call such a triangle as a *filled* triangle), the other two links would generate no energy gain from the second-order processes because these two unoccupied links are simultaneously connected to one end of a nearby dimer, generating a "perpendicular" arrangement between the filled link of a triangle and a nearby dimer. Hence if we denote the number of the filled triangles as $N_{\text{filled}\Delta}$, the number of the unoccupied links that connect two nearby dimers in parallel configuration is $N_{\text{Link}}-N_{\text{Dimer}}-2N_{\text{filled}\Delta}$. Therefore, the total-energy gain per spin from the second-order processes is given by

$$\Delta E^{(2)}=\Delta\epsilon^{(2)}\left\{\frac{N_{\text{Link}}-N_{\text{Dimer}}-2N_{\text{filled}\Delta}}{N}\right\}=\Delta\epsilon^{(2)}\left\{1-2\frac{N_{\text{filled}\Delta}}{N}\right\}. \quad (1)$$

Note that the condition $N_{\text{filledg}\Delta}=0$ uniquely determines the ground-state VBS configuration which is shown in Fig. 2(a). Here the unit cell consists of six dimer singlets which lie in a pinwheel structure and we call this VBS state as the VBS-12 state. In the VBS-12, every triangle is an *empty* triangle, that is, no link of a triangle is occupied by a dimer singlet. This is the dimer configuration one would obtain when only J_1 is present or $J_2, J_3 \ll J_1$ [see Fig. 1(a)]. It is interesting to note that the VBS-12 state is stable all the way to the limit where J_2 and J_3 become comparable to J_1.

B. Third-order perturbation and the VBS-36 state

Now we extend the perturbation theory to the third order in λ. Let us first consider two neighboring dimers lying in parallel as shown in Fig. 4(a). In addition to the energy gain from the second-order perturbation, $\Delta\epsilon^{(2)}$, this local configuration allows a third-order process which results in the energy gain, $\Delta\epsilon_a^{(3)}=-\frac{3}{128}J\lambda^3$. On the other hand, the dimer configuration in Fig. 4(b) does not allow any third-order process. In fact, this configuration is locally an eigenstate of the Hamiltonian and does not produce any virtual state in any order of the perturbation theory. Similarly, the unoccupied links in Fig. 4(c) making an *empty* triangle would not generate any energy gain in the third order either. Therefore when we calculate the third-order energy gain coming from various local configurations, we have to remember that the unoccupied links on every filled and empty triangles would not produce any third-order energy shift.

Figure 4(d) shows another configuration in which a new third-order process can be generated. This structure, which is commonly known as a *perfect* hexagon, consists of three neighboring dimers lying on a hexagon. Through the resonating third-order processes around a perfect hexagon, the ground-state energy can be lowered by $\Delta\epsilon_b^{(3)}=-\frac{9}{128}J\lambda^3$.

Based on these results, the total-energy gain per spin by the third-order processes can be summarized as follows:

$$\Delta E^{(3)}=\Delta\epsilon_a^{(3)}\left\{\frac{N_{\text{Link}}-N_{\text{Dimer}}-2N_{\text{filled}\Delta}-3N_{\text{empty}\Delta}}{N}\right\}+\Delta\epsilon_b^{(3)}\frac{N_{\text{perfect}}}{N}=\Delta\epsilon_a^{(3)}\left\{\frac{1}{2}+\frac{N_{\text{filled}\Delta}}{N}\right\}+\Delta\epsilon_b^{(3)}\frac{N_{\text{perfect}}}{N}, \quad (2)$$

where N_{perfect} represents the number of perfect hexagons, and

we use the fact that the number of triangles, $N_\Delta = N/6$, satisfies $N_\Delta = N_{\text{empty}\Delta} + N_{\text{filled}\Delta}$.

Therefore if we can maximize the number of the filled triangles and perfect hexagons, we can get the largest energy gain from the third-order processes. The VBS-36 state depicted in Fig. 2(b) satisfies this requirement, that is, $N_{\text{filled}\Delta} = N_\Delta$ and $N_{\text{perfect}} = \frac{2}{3} N_{\text{Hexagon}}$. Note that the three neighboring hexagons lying in a triangular structure cannot be perfect at the same time for any kind of dimer coverings. Interestingly, this VBS-36 phase is adiabatically connected to the 36-site-unit-cell VBS ground state of the ideal kagome lattice[8,9] in the sense that as we increase the magnitude of J_4/J from zero to one, the VBS-36 phase evolves smoothly to the 36-site-unit-cell VBS ground state of the ideal kagome lattice.

In the case of the J_4-depleted lattice, the VBS ground state is already uniquely determined by the second-order perturbation theory. That is, the VBS-12 phase is the ground state and the VBS-36 phase is a closely competing phase. However, it is not clear which phase is more stable when J_4 has finite magnitude. In the case of the ideal kagome lattice, all the dimer coverings are degenerate up to the second order in λ and the degeneracy can only be lifted by the third-order perturbation processes as emphasized in Ref. 9. This is because the numbers of the filled and empty triangles on the ideal kagome lattice are fixed for any dimer covering due to the spatial geometry of the ideal kagome lattice (see Ref. 8). This is, in fact, the reason why the 36-site-unit-cell VBS is the most stable VBS state on the ideal kagome lattice. Therefore, we may expect that the change in magnitude of J_4 would affect the relative importance between the second-order and the third-order processes. In the next section, we investigate the effect of finite J_4 on the ground-state properties of the deformed kagome lattice.

III. VALENCE BOND SOLID PHASES OF THE DEFORMED KAGOME ANTIFERROMAGNET: THE EFFECT OF FINITE J_4

A. Dimer series expansion study

In order to refine the ground-state energy estimation beyond the third-order perturbation theory and confirm the results of the previous lowest-order expansions, we develop a systematic scheme to compute the perturbation series using the linked cluster expansion method. In this approach, the ground-state energy can be expressed as the sum of the contributions from a sequence of finite clusters.[22,23] To carry out the series expansion, all the occupied links that make up the dimer covering are given an interaction strength J and all the other unoccupied links are given a strength λJ. We apply the series expansion method to compute the energy of the two competing VBS phases on the J_4-depleted lattice, $J_4=0$, and the ideal kagome lattice limit, $J_4/J=1$, up to the fifth order in λ.

The ground-state energy per site of an infinite lattice can be written as a sum over cluster terms of the form, $E_0/N = \Sigma_g c(g)\varepsilon(g)$. Here $c(g)$ is the so-called lattice constant for the cluster g, which is the number of embeddings of the cluster g per lattice site. $\varepsilon(g)$ is the reduced energy of the cluster g, which is defined recursively as $\varepsilon(g) = E(g) - \Sigma_{g'} c(g'/g)\varepsilon(g')$. Here $E(g)$ is the ground-state energy of the cluster g, and the sum is over all subclusters g' of g. Since the reduced energy $\varepsilon(g)$ is equal to the sum of the contributions from all connected diagrams (i.e., the patterns of connected dimers) that span the cluster g, such diagrams only contribute beyond a certain minimum order in λ, proportional to the size of the cluster. Thus, to obtain a perturbation series that is exact up to a given order, it is sufficient to sum up the reduced energies of all the clusters up to the corresponding size. This gives us a systematic procedure for carrying out the expansion to higher orders.[22]

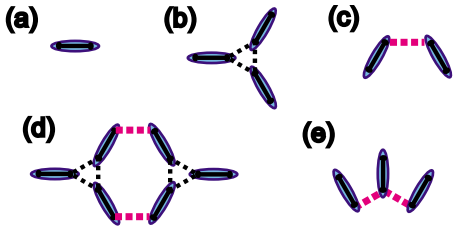

FIG. 5. (Color online) Topologies of the graphs (diagrams) relevant to the VBS-12 phase on the J_4-depleted kagome lattice that contribute to the ground-state energy up to the fifth order in λ. The thick dotted (pink) lines are the weak links on the hexagons, while the thin dotted (black) links represent the weak links on the empty triangles.

Another appealing aspect of applying the linked cluster expansion method is that we can considerably reduce the complexity of the calculation by using the freedom in choosing clusters.[24,25] In a recent work of the dimer series expansion study on the ideal kagome lattice,[9] the unoccupied links on each triangle are grouped together, which results in significant simplification of the computation and rapid convergence of the series for the ground-state energy. In this scheme, for any dimer covering on the ideal kagome lattice, every empty and filled triangles constitute the elementary clusters. All the other clusters can be constructed by putting the elementary clusters together appropriately. Based on this specially designed clusters, it was shown that the series for the ground-state energy can be determined up to the fifth order in λ using only five different graphs (or diagrams).[9] Summing up the terms in the series, the ground-state energy per spin of the VBS-36 phase on the ideal kagome lattice is estimated to be $-0.432J$. For comparison, we compute the ground-state energy of the VBS-12 phase on the ideal kagome lattice. The same graphs can be used for the calculation and the summation of the terms in the series up to the fifth order in λ leads to the energy of $-0.424J$. Note that even though the VBS phase with a 36-site unit cell is the ground state of the ideal kagome lattice, the energy difference between the two VBS phases is quite small.

Applying similar strategies to the J_4-depleted kagome lattice, we compute the series for the ground-state energy of the two competing VBS phases. We first consider the VBS-12 phase on the J_4-depleted kagome lattice. Here we group the three weak links on an empty triangle together and distinguish them from the other weak links on the hexagons. In this scheme, only five different graphs (shown in Fig. 5) contribute to the ground-state energy up to the fifth order in

λ. The smallest cluster in Fig. 5(a) is made of a single dimer and has the reduced energy, $\varepsilon_{0,a}=-\frac{3}{4}J$. Figures 5(b) and 5(c) show two clusters whose contributions start from the second order in λ. The reduced energies of the corresponding clusters, i.e., $\varepsilon_{2,b}$ and $\varepsilon_{2,c}$ respectively, can be obtained after subtracting the subcluster energy $\varepsilon_{0,a}$ appropriately and are found to be

$$\frac{\varepsilon_{2,b}}{J}=-\frac{9}{32}\lambda^2+0.039\ 550\ 78\lambda^4-0.011\ 123\ 66\lambda^6+O(\lambda^8),$$

$$\frac{\varepsilon_{2,c}}{J}=-\frac{3}{32}\lambda^2-\frac{3}{128}\lambda^3-\frac{3}{2048}\lambda^4+\frac{15}{8192}\lambda^5+O(\lambda^6).$$

Finally, the resonance processes coming from the remaining two graphs in Figs. 5(d) and 5(e) can lower the ground-state energy through the fourth-order processes. The corresponding reduced energies of the two clusters, i.e., $\varepsilon_{4,d}$ and $\varepsilon_{4,e}$ can be obtained by the same procedure used earlier and using the fact that the subclusters are made of the graphs in Figs. 5(a)–5(c). Since the reduced energies of all the other clusters that are larger in size than those in Figs. 5(d) and 5(e), begin with $O(\lambda^6)$ terms, the ground-state energy can be determined exactly at least up to the fifth order in λ with those five graphs shown in Fig. 5. After we determine the lattice constants of all the clusters, the ground-state energy for the infinite lattice is found to be

$$\frac{E_0}{J}=-\frac{3}{8}-\frac{3}{32}\lambda^2-\frac{3}{256}\lambda^3-0.009\ 765\ 6\lambda^4-0.007\ 975\ 3\lambda^5.$$

This leads to the estimation of the ground-state energy, $-0.498J$ for the VBS-12 phase.

Following similar procedures, the ground-state energy of the VBS-36 phase is obtained as

$$\frac{E_0}{J}=-\frac{3}{8}-\frac{1}{16}\lambda^2-\frac{5}{256}\lambda^3-0.010\ 742\ 2\lambda^4-0.005\ 514\ 1\lambda^5.$$

This leads to the estimation of the ground-state energy, $-0.473J$ for the VBS-36 phase, which is higher than that of the VBS-12 state. This is consistent with the previous results of the perturbation theory, and the VBS-12 phase is the ground state of the J_4-depleted kagome lattice.

In summary, the VBS-12 phase is lower in energy on the J_4-depleted kagome lattice ($J_4=0$), while the VBS-36 phase has lower energy on the ideal kagome lattice ($J_4=1$). Based on this result, we expect that there should be an energy level crossing between these two limits as the magnitude of J_4/J is changed from zero to one. In order to obtain the detailed information about the level crossing, we use the self-consistent bond operator mean-field approach to the two phases for an arbitrary strength of J_4/J in the next section.

B. Bond operator mean-field theory

We study the relative stability of the VBS-12 and VBS-36 phases using the bond operator mean-field theory[26–28] for the deformed kagome lattice with an arbitrary strength of $J_4/J \leq 1$. In this formulation, the dimer singlet degrees of freedom are used as natural building blocks and the quantum corrections coming from the triplet fluctuations can systematically be investigated.[29,30]

Let us consider the two $S=\frac{1}{2}$ spins constituting a dimer singlet, $\mathbf{S}_R$ and $\mathbf{S}_L$. The Hilbert space is spanned by four states that can be taken as a singlet state, $|s\rangle$, and three triplet states, $|t_x\rangle$, $|t_y\rangle$, and $|t_z\rangle$. Then, the singlet and triplet boson operators are introduced such that each of the above states can be created from the vacuum $|0\rangle$ as follows:

$$|s\rangle=s^\dagger|0\rangle=\frac{1}{\sqrt{2}}(|\uparrow\downarrow\rangle-|\downarrow\uparrow\rangle),$$

$$|t_x\rangle=t_x^\dagger|0\rangle=-\frac{1}{\sqrt{2}}(|\uparrow\uparrow\rangle-|\downarrow\downarrow\rangle),$$

$$|t_y\rangle=t_y^\dagger|0\rangle=\frac{i}{\sqrt{2}}(|\uparrow\uparrow\rangle+|\downarrow\downarrow\rangle),$$

$$|t_z\rangle=t_z^\dagger|0\rangle=\frac{1}{\sqrt{2}}(|\uparrow\downarrow\rangle+|\downarrow\uparrow\rangle).$$

To eliminate unphysical states from the enlarged Hilbert space, the following constraint needs to be imposed on the bond-particle Hilbert space:

$$s^\dagger s+t_\alpha^\dagger t_\alpha=1,$$

where $\alpha=x$, y, and z, and we adopt the summation convention for the repeated indices hereafter unless mentioned otherwise.

Constrained by this equation, the exact expressions for the spin operators can be written in terms of the bond operators:

$$S_{R\alpha}=\frac{1}{2}(s^\dagger t_\alpha+t_\alpha^\dagger s-i\varepsilon_{\alpha\beta\gamma}t_\beta^\dagger t_\gamma),$$

$$S_{L\alpha}=\frac{1}{2}(-s^\dagger t_\alpha-t_\alpha^\dagger s-i\varepsilon_{\alpha\beta\gamma}t_\beta^\dagger t_\gamma),$$

where $\varepsilon_{\alpha\beta\gamma}$ is the third-rank totally antisymmetric tensor with $\varepsilon_{xyz}=1$.

We consider the antiferromagnetic Heisenberg model Hamiltonian, $H=\Sigma_{\langle ij\rangle}J_{ij}\mathbf{S}_i\cdot\mathbf{S}_j$, where the exchange couplings of the neighboring spins are taken to be $J_1=J_2=J_3=J\geq J_4$ (see Fig. 1). Utilizing the bond operator representation of spin operators, the Hamiltonian can be rewritten solely in terms of bond-particle operators. The hardcore constraint among bond-particle operators is imposed via the Lagrange multiplier method. The quartic interactions between the triplets in the resulting Hamiltonian are treated by the self-consistent Hartree-Fock approximation.

The computational procedure for the VBS-36 phase is basically in parallel to that of the recent work on the 36-site-unit-cell VBS ground state of the ideal kagome lattice.[31] Here we present some details of the bond operator theory applied to the VBS-12 phase on the deformed kagome lattice. Since the six dimers within the unit cell of the VBS-12 phase are equivalent as is obvious from the sixfold rotational

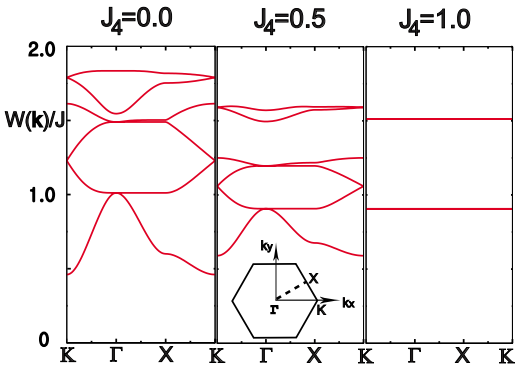

FIG. 6. (Color online) Evolution of the triplet dispersion spectra of the VBS-12 phase as a function of J_4/J (J is set to one). Note that the lower flat mode is fourfold degenerate, while the upper one is doubly degenerate when $J_4/J=1$

symmetry of the ordering pattern in Fig. 2(a), the singlet condensate density $\langle s_{\mathbf{i},n}\rangle$ and the chemical potential $\mu_{\mathbf{i},n}$ can be set to be $\langle s_{\mathbf{i},n}\rangle=\bar{s}$ and $\mu_{\mathbf{i},n}=\mu$ in our mean-field theory. Here $\mathbf{i}$ denotes the position of the unit cell and n indicates the dimer index inside the unit cell. The hard-core constraint on the bond-particle operators is imposed by adding the following Lagrange multiplier term: $H_\mu=-\Sigma_{\mathbf{i},n}\mu(\bar{s}^2+t^\dagger_{\mathbf{i},n\alpha}t_{\mathbf{i},n\alpha}-1)$.

The quartic interactions between the triplet particles are decoupled using the mean-field order parameters P_γ and Q_γ, where $P_\gamma\equiv\langle t^\dagger_{\mathbf{i},n\alpha}t_{\mathbf{j},m\alpha}\rangle$ and $Q_\gamma\equiv\langle t_{\mathbf{i},n\alpha}t_{\mathbf{j},m\alpha}\rangle$. We consider four mean-field variables, P_γ and Q_γ, labeled by $\gamma=1$ or 2. Here P_1 and Q_1 denote the diagonal and off-diagonal triplet correlations between the dimers residing in the *same* unit cell while the other two variables P_2 and Q_2 represent the triplet correlations between neighboring dimers in *different* unit cells. The above four order parameters P_1, Q_1, P_2, and Q_2 together with $\bar{s}$ and μ are determined self-consistently by solving the coupled saddle-point equations.[27,28]

In Fig. 6, we plot the ground-state energies of the VBS-12 and VBS-36 phases as a function of $0\leq J_4/J\leq 1$. When $J_4=0$, the ground-state energy of the VBS-12 (VBS-36) from the bond operator mean-field theory is $-0.496J$ ($-0.470J$) which is close to the results from the series expansion study, $-0.498J$ ($-0.473J$). As one increases the magnitude of J_4, the ground-state energy of the VBS-12 grows more rapidly than that of the VBS-36 phase, and finally an energy level crossing occurs around $J_4=0.97J$. Beyond this point the VBS-36 phase becomes more stable and remains as the ground state up to the ideal kagome lattice limit.

The evolution of the triplet excitation spectrum for the VBS-12 phase shows interesting behavior as the magnitude of J_4 changes. In Fig. 3, we plot the triplet dispersion spectra when $J_4=0$, 0.5 and 1, respectively. Note that the triplet dispersion of the VBS-12 phase on the ideal kagome lattice ($J_4=J$) shows completely flat spectrum. Flat dispersion in the momentum space indicates the existence of localized eigenstates.[31] In this case, the three neighboring dimers around an empty triangle support the localized eigenmodes. When $J_4=J$, the six dimers within a unit cell are all "orthogonal" to each other in the sense that each spin of a dimer is simultaneously connected to the two spins of its neighboring dimers as shown in Fig. 2(a). In this situation, the triplet particles can fluctuate only through the dimers of its neighboring unit cell connected via empty triangles, and hence they are confined within that space. The three localized triplet modes coming from the three dimers around an empty triangle consist of doubly degenerate E modes and a nondegenerate A mode (in the standard convention of irreducible representations in group theory[32]). Since the unit cell consists of six dimers, each E mode and A mode is doubly degenerate. In Fig. 3(c), the lower flat mode has fourfold degeneracy while the upper one is doubly degenerate.

The fact that all the triplet dispersions are completely flat is an interesting characteristic of the triplet spectrum of the VBS-12 phase on the ideal kagome lattice (note, however, that the true ground state is the VBS-36 phase on the ideal kagome lattice). According to a recent work,[31] the triplet spectra of the VBS-36 phase on the ideal kagome lattice contain some dispersive modes even though the number of flat modes is quite large there as well. In particular, the lowest flat band is degenerate with the second lowest dispersive band only at the zone center. As discussed in detail in Refs. 31 and 33, the degeneracy at a particular momentum point reflects the existence of noncontractible loop states and is topologically protected. Therefore, the completely flat spectrum of the VBS-12 phase on the ideal kagome lattice means that all the flat modes are topologically trivial. This results from the fact that the size of every localized mode is not larger than the size of the unit cell and each localized eigenmode around an empty triangle is linearly independent. The condition for the emergence of the topologically nontrivial structure in dispersions is discussed in detail in Ref. 33. (See also Ref. 31.)

On the other hand, when the magnitude of J_4 is reduced, the degenerate bands split and triplet particles spread over the whole lattice. In the case of $J_4=0.5J$ that may directly be relevant to $Rb_2Cu_3SnF_{12}$, one can still see the gap between the lower four bands and the upper two bands. However, when J_4 becomes vanishingly small, the gap structure disappears due to wide bandwidth of the triplet bands.

IV. DISCUSSION

In the case of the VBS phases with a big unit cell, a large number of degenerate dimer configurations may allow many singlet excitations below a spin gap. For example, the VBS-36 order on the ideal kagome lattice leads to the large degeneracy that comes from the combination of the broken translational symmetry and the local resonance moves around flippable loops (see Refs. 8 and 10). Here the flippable loops mean a collection of alternating occupied and unoccupied links; when the roles of the occupied and unoccupied links on a flippable loop are interchanged, one hard-core dimer covering can be continuously transformed to another one. The perfect hexagons and the pinwheel dimers form the smallest flippable loops in the case of the 36-site VBS phase on the ideal kagome lattice.[8] The number of singlet excitations arising from such considerations is still smaller than what was observed in the exact diagonalization studies[34–37] of small system sizes (up to 36 sites) for the spin-1/2 antiferromagnetic Heisenberg model on the ideal

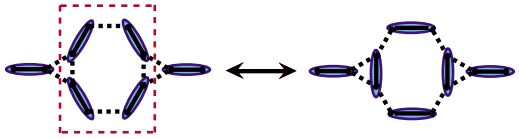

FIG. 7. (Color online) A local singlet resonance in the VBS-12 phase on the J_4-depleted kagome lattice. Here the dotted (red) square represents the smallest flippable loop.

kagome lattice. It was, however, argued that the triplets can scatter to form additional singlet bound states in finite-size systems and this may explain the exact diagonalization results.[10]

On the other hand, the VBS-12 phase on the J_4-depleted kagome lattice does not break any translational symmetry and the local resonances from loop flips are the only sources of low-energy singlet excitations. In Fig. 7, we show the smallest flippable loop consisting of the four occupied and four unoccupied links, and its loop flip in the VBS-12 phase. Note that there is a change in the number of the empty and filled triangles after the loop flips. In fact, a single loop flip increases the number of the filled triangles by two. According to Eqs. (1) and (2) in the perturbation theory, this requires the energy cost of $-4\Delta\epsilon^{(2)}+2\Delta\epsilon_a^{(3)}=\frac{21}{64}J$, which is much larger than the measured spin gap ~ 20 K if the experimentally estimated $J\sim 200$ K is used. Since the number of the filled triangles involved in a loop flip is proportional to the size of the flippable loop, the singlet excitations coming from a larger loop flip require even higher-energy cost. Therefore, the VBS-12 phase is quite stable against local singlet fluctuations and it seems difficult to produce "the singlet wave" whose existence is speculated in a recent experimental paper.[20] We expect the lowest singlet excitation would be well above the spin gap, which can be contrasted with many singlet excitations below a spin gap in the case of the ideal kagome lattice.

In summary, slight lattice distortions can completely change the nature of the ground state of the quantum antiferromagnet on the kagome lattice, and this leads to the abrupt modification of the elementary excitation spectra in both the triplet and singlet channels. Even though J_1, J_2, and J_3 are not exactly the same in $Rb_2Cu_3SnF_{12}$, the magnitudes of these exchange couplings are very similar and satisfy $J_1 > J_2 > J_3 \gg J_4$. Interestingly, the VBS-12 phase studied in this work corresponds to the dimer covering that resides only on the J_1 links. This suggests that the VBS-12 phase on the J_1 links is stable all the way to the limit where J_2 and J_3 become the same as J_1. Thus, we expect that our results are directly applicable to $Rb_2Cu_3SnF_{12}$. In particular, our predictions on the triplet and singlet spectra can be tested in the future neutron-scattering and specific-heat experiments on $Rb_2Cu_3SnF_{12}$.

ACKNOWLEDGMENTS

We thank Tyler Dodds, Michael J. Lawler, Kwon Park, and Erik S. Sørensen for helpful discussions. This work was supported by the NSERC of Canada, the Canada Research Chair, and the Canadian Institute for Advanced Research.

[1] G. Misguich and C. Lhuillier, in *Frustrated Spin Systems*, edited by H. T. Diep (World Scientific, Singapore, 2004), pp. 229–306.
[2] S. Sachdev, Phys. Rev. B **45**, 12377 (1992).
[3] F. Wang and A. Vishwanath, Phys. Rev. B **74**, 174423 (2006).
[4] M. B. Hastings, Phys. Rev. B **63**, 014413 (2000).
[5] Y. Ran, M. Hermele, P. A. Lee, and X. G. Wen, Phys. Rev. Lett. **98**, 117205 (2007).
[6] S. Ryu, O. I. Motrunich, J. Alicea, and M. P. A. Fisher, Phys. Rev. B **75**, 184406 (2007).
[7] J. B. Marston and C. Zeng, J. Appl. Phys. **69**, 5962 (1991).
[8] P. Nikolic and T. Senthil, Phys. Rev. B **68**, 214415 (2003).
[9] R. R. P. Singh and D. A. Huse, Phys. Rev. B **76**, 180407(R) (2007).
[10] R. R. P. Singh and D. A. Huse, Phys. Rev. B **77**, 144415 (2008).
[11] F. Wang, A. Vishwanath, and Y. B. Kim, Phys. Rev. B **76**, 094421 (2007).
[12] M. J. Lawler, L. Fritz, Y. B. Kim, and S. Sachdev, Phys. Rev. Lett. **100**, 187201 (2008).
[13] N. Rogado, M. K. Haas, G. Lawes, D. A. Huse, A. P. Ramirez, and R. J. Cava, J. Phys.: Condens. Matter **15**, 907 (2003).
[14] Y. Yamabe, T. Ono, T. Suto, and H. Tanaka, J. Phys.: Condens. Matter **19**, 145253 (2007).
[15] Y. Okamoto, H. Yoshida, and Z. Hiroi, J. Phys. Soc. Jpn. **78**, 033701 (2009).
[16] M. P. Shores, E. A. Nytko, B. M. Bartlett, and D. G. Nocera, J. Am. Chem. Soc. **127**, 13462 (2005).
[17] J. S. Helton, K. Matan, M. P. Shores, E. A. Nytko, B. M. Bartlett, Y. Yoshida, Y. Takano, A. Suslov, Y. Qiu, J.-H. Chung, D. G. Nocera, and Y. S. Lee, Phys. Rev. Lett. **98**, 107204 (2007).
[18] P. Mendels, F. Bert, M. A. de Vries, A. Olariu, A. Harrison, F. Duc, J. C. Trombe, J. S. Lord, A. Amato, and C. Baines, Phys. Rev. Lett. **98**, 077204 (2007).
[19] Z. Hiroi, M. Hanawa, N. Kobayashi, H. Takagi, Y. Kato, and M. Takigawa, J. Phys. Soc. Jpn. **70**, 3377 (2001).
[20] K. Morita, M. Yano, T. Ono, H. Tanaka, K. Fugii, H. Uekusa, Y. Narumi, and K. Kindo, J. Phys. Soc. Jpn. **77**, 043707 (2008).
[21] T. Barnes, J. Riera, and D. A. Tennant, Phys. Rev. B. **59**, 11384 (1999).
[22] J. Oitmaa, C. Hamer, and W.-H. Zheng, *Series Expansion Methods for Strongly Interacting Lattice Models* (Cambridge University Press, Cambridge, 2006).
[23] C. Domb and M. S. Green, *Phase Transitions and Critical Phenomena* (Academic Press, New York, 1974), Vol. 3.
[24] M. Rigol, T. Bryant, and R. R. P. Singh, Phys. Rev. E **75**, 061118 (2007).
[25] M. Rigol, T. Bryant, and R. R. P. Singh, Phys. Rev. Lett. **97**, 187202 (2006).
[26] A. V. Chubukov, JETP Lett. **49**, 129 (1989).
[27] S. Sachdev and R. N. Bhatt, Phys. Rev. B **41**, 9323 (1990).
[28] S. Gopalan, T. M. Rice, and M. Sigrist, Phys. Rev. B **49**, 8901

(1994).
[29] V. N. Kotov, O. Sushkov, Z. Weihong, and J. Oitmaa, Phys. Rev. Lett. **80**, 5790 (1998).
[30] O. P. Sushkov and V. N. Kotov, Phys. Rev. Lett. **81**, 1941 (1998).
[31] B.-J. Yang, Y. B. Kim, J. Yu, and K. Park, Phys. Rev. B **77**, 224424 (2008).
[32] M. Tinkham, *Group Theory and Quantum Mechanics* (McGraw-Hill, New York, 1964).
[33] D. L. Bergman, C. Wu, and L. Balents, Phys. Rev. B **78**, 125104 (2008).
[34] P. Lecheminant, B. Bernu, C. Lhuillier, L. Pierre, and P. Sindzingre, Phys. Rev. B **56**, 2521 (1997).
[35] Ch. Waldtmann, H.-U. Everts, B. Bernu, C. Lhuillier, P. Sindzingre, P. Lecheminant, and L. Pierre, Eur. Phys. J. B **2**, 501 (1998).
[36] G. Misguich and B. Bernu, Phys. Rev. B **71**, 014417 (2005).
[37] G. Misguich and P. Sindzingre, J. Phys.: Condens. Matter **19**, 145202 (2007).